Integrin-targeted cancer immunotherapy elicits protective adaptive immune responses

Integrin-targeted cancer immunotherapy elicits protective adaptive immune responses

Byron H. Kwan,[1,2] Eric F. Zhu,[2,3] Alice Tzeng,[1,2] Harun R. Sugito,[1,2] Ahmed A. Eltahir,[2,4] Botong Ma,[2,5] Mary K. Delaney,[2,3,4] Patrick A. Murphy,[2,6] Monique J. Kauke,[2,3] Alessandro Angelini,[2] Noor Momin,[1,2] Naveen K. Mehta,[1,2] Alecia M. Maragh,[1,2] Richard O. Hynes,[2,6] Glenn Dranoff,[7] Jennifer R. Cochran,[8,9] and K. Dane Wittrup[1,2,3]

[1]Department of Biological Engineering, [2]Koch Institute for Integrative Cancer Research, [3]Department of Chemical Engineering, [4]Department of Biology, [5]Department of Mathematics, and [6]Howard Hughes Medical Institute, Massachusetts Institute of Technology, Cambridge, MA 02139
[7]Novartis Institutes for BioMedical Research, Cambridge, MA 02139
[8]Department of Bioengineering and [9]Department of Chemical Engineering, Stanford University, Stanford, CA 94305

Certain RGD-binding integrins are required for cell adhesion, migration, and proliferation and are overexpressed in most tumors, making them attractive therapeutic targets. However, multiple integrin antagonist drug candidates have failed to show efficacy in cancer clinical trials. In this work, we instead exploit these integrins as a target for antibody Fc effector functions in the context of cancer immunotherapy. By combining administration of an engineered mouse serum albumin/IL-2 fusion with an Fc fusion to an integrin-binding peptide (2.5F-Fc), significant survival improvements are achieved in three syngeneic mouse tumor models, including complete responses with protective immunity. Functional integrin antagonism does not contribute significantly to efficacy; rather, this therapy recruits both an innate and adaptive immune response, as deficiencies in either arm result in reduced tumor control. Administration of this integrin-targeted immunotherapy together with an anti–PD-1 antibody further improves responses and predominantly results in cures. Overall, this well-tolerated therapy achieves tumor specificity by redirecting inflammation to a functional target fundamental to tumorigenic processes but expressed at significantly lower levels in healthy tissues, and it shows promise for translation.

INTRODUCTION

Recent clinical outcomes and subsequent approvals of anti–CTLA-4 and anti–PD-1 checkpoint blockade antibodies, which mitigate inhibitory signaling that decreases antitumor T cell responses, have ignited extraordinarily broad efforts to develop the potential of cancer immunotherapy (Pardoll, 2012; Topalian et al., 2015). Unlike strategies that typically elicit antitumor responses of limited duration and nearly inevitable treatment resistance, immunotherapeutics can achieve durable and long-lasting antitumor responses in a minority of patients with advanced disease (Sharma and Allison, 2015). To build upon this success, combination immunotherapies are a next logical step (Gajewski et al., 2013; Spranger and Gajewski, 2013).

One such approach combines a tumor-specific antibody to drive antibody-dependent cell-mediated cytotoxicity (ADCC) through neutrophil- and eosinophil-mediated attack and an extended serum half-life IL-2 fusion to activate $CD8^+$ T cells and NK cells. However, this strategy is limited to antibodies against validated tumor-associated antigens, for which only a handful of marketed clinical agents are available (e.g., rituximab, cetuximab, trastuzumab). Furthermore, there are very few established murine model systems for fundamental study of antibody immunotherapy in the presence of an intact immune system (Zhu et al., 2015).

To address this issue, we investigated the possibility of using integrins as a general tumor target. Integrins are a family of α-β heterodimeric cell surface receptors functionally required for cell adhesion, migration and proliferation (Hynes, 1992, 2002). The RGD-binding subclass of integrins, particularly $\alpha_5\beta_1$ and integrins containing α_v, are overexpressed in many tumor cells and their vasculature and thus have been a focus of anticancer efforts (Hood and Cheresh, 2002; Desgrosellier and Cheresh, 2010; Weis and Cheresh, 2011b). Unfortunately, all prior integrin-targeted cancer therapies, which have primarily sought to antagonize integrin function in tumors, failed in clinical trials because of lack of efficacy (Hersey et al., 2010; O'Day et al., 2011; Goodman and Picard, 2012; Heidenreich et al., 2013; Stupp et al., 2014). Because integrin expression switching among different RGD-binding integrins is a potential mechanism by which tumors can evade treatment, particularly between α_v and α_5 or β_1 and β_3 (van der Flier et al., 2010; Parvani et al., 2013; Sheldrake and Patterson, 2014), it is important to note that unsuccessful clinical candidates recognized either the α_v subunit or $\alpha_5\beta_1$,

Correspondence to K. Dane Wittrup: wittrup@mit.edu

Abbreviations used: CBC, complete blood count; MSA, mouse serum albumin.

The Rockefeller University Press $30.00
J. Exp. Med. 2017 Vol. 214 No. 6 1679–1690
https://doi.org/10.1084/jem.20160831

Supplemental material can be found at:
http://doi.org/10.1084/jem.20160831

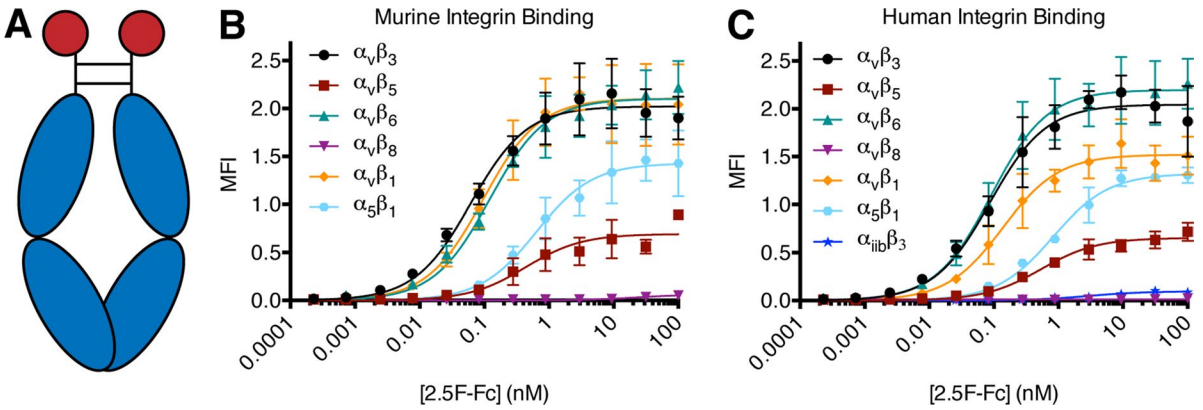

Figure 1. **A fusion between a species–cross-reactive integrin-binding peptide and an Fc domain results in an antibody-like construct (2.5F-Fc) capable of targeting various RGD-binding integrins.** (A) Schematic of the structure of 2.5F-Fc, consisting of the integrin-binding peptide (red) fused to the Fc domain (blue) through the hinge region (black). (B and C) ELISA measuring binding of 2.5F-Fc to various (B) murine and (C) human RGD-binding integrins. Symbols and error bars represent means ± SD (n = 3). B and C represent data from three pooled independent experiments.

but not both (Desgrosellier and Cheresh, 2010; Goodman and Picard, 2012). Furthermore, certain doses of RGD-mimetic inhibitors can counterintuitively increase tumor angiogenesis and growth, suggesting that direct functional integrin antagonism is unlikely to prove a viable treatment strategy (Reynolds et al., 2009).

Nevertheless, these RGD-binding integrins are a highly validated tumor-associated antigen and, in this work, we used them as a target for recruiting immune effector functions in combination with MSA/IL-2, a mouse serum albumin (MSA)–IL-2 fusion with extended half-life in serum. The engineered integrin-targeting cysteine knot peptide, 2.5F, has been described previously as a highly specific imaging agent for the detection of various tumors (Kimura et al., 2009a,b; Nielsen et al., 2010; Moore et al., 2013). Using 2.5F, we generated an Fc fusion (2.5F-Fc) that was able to control tumor growth in three syngeneic murine models of cancer in combination with MSA/IL-2. We demonstrated that this integrin-targeted combination immunotherapy did not exert tumor control through functional integrin antagonism or vascular disruption but instead was critically dependent on recruiting both innate and adaptive immune responses. Finally, we determined that the addition of anti–PD-1 therapy to this combination further improves therapeutic responses and predominantly results in cures.

RESULTS

2.5F-Fc is an antibody-like construct highly cross-reactive against multiple human and murine integrins

The aforementioned 2.5F peptide was fused to the hinge region of the murine IgG2a Fc domain, forming an antibody-like construct where the Fab regions are replaced by the 2.5F peptide (Fig. 1 A). The murine IgG2a Fc isotype was chosen because it is the most activating of the murine Fc isotypes (Nimmerjahn and Ravetch, 2005). 2.5F-Fc recognizes five different RGD-binding murine and human integrins: $\alpha_v\beta_1$, $\alpha_v\beta_3$, $\alpha_v\beta_5$, $\alpha_v\beta_6$, and $\alpha_5\beta_1$ (Fig. 1, B and C), of which the latter four have been shown to be highly overexpressed in various cancers (Hood and Cheresh, 2002; Desgrosellier and Cheresh, 2010; Weis and Cheresh, 2011b).

MSA/IL-2 and 2.5F-Fc synergistically control tumors in three syngeneic models of cancer

To explore the therapeutic potential of 2.5F-Fc when combined with MSA/IL-2, we tested their antitumor efficacy against syngeneic mouse models of cancer. This combination achieved synergistic survival improvements in mice bearing 6 d B16F10 melanoma, Ag104A fibrosarcoma, and MC38 colon carcinoma flank tumors (Fig. 2, A–C; and Fig. S1, A–C). Importantly, the combination of both agents was required, as MSA/IL-2 and 2.5F-Fc are each ineffective as monotherapy. When MC38-bearing mice cured by this therapy were rechallenged with MC38 cells at a distal site, the resulting tumor demonstrated significantly retarded growth or was completely unable to establish, indicating protective immunity as a consequence of treatment (Fig. 2 D and Fig. S1 D).

Integrin-targeted immunotherapy is well tolerated in mice

Because previous imaging studies with 2.5F accomplish almost exclusive tumor localization (Kimura et al., 2009a; Nielsen et al., 2010; Moore et al., 2013), integrin-targeted immunotherapy was, not surprisingly, well tolerated in the mice. Treated mice gained weight and exhibited good body condition (Fig. 3 A). Mice treated with MSA/IL-2 + 2.5F-Fc (but not those treated with the single agents) exhibited a transient and reversible increase in serum alanine transaminase and decrease in albumin, indicating short-lived effects of treatment on liver function (Fig. 3, B and C). Minimal changes in blood urea nitrogen occurred, suggesting normal kidney function throughout treatment (Fig. 3 D). Histopathological analysis indicated that IL-2 is a primary driver of transient inflammation in both the liver and the lung (Fig. S2), consistent with

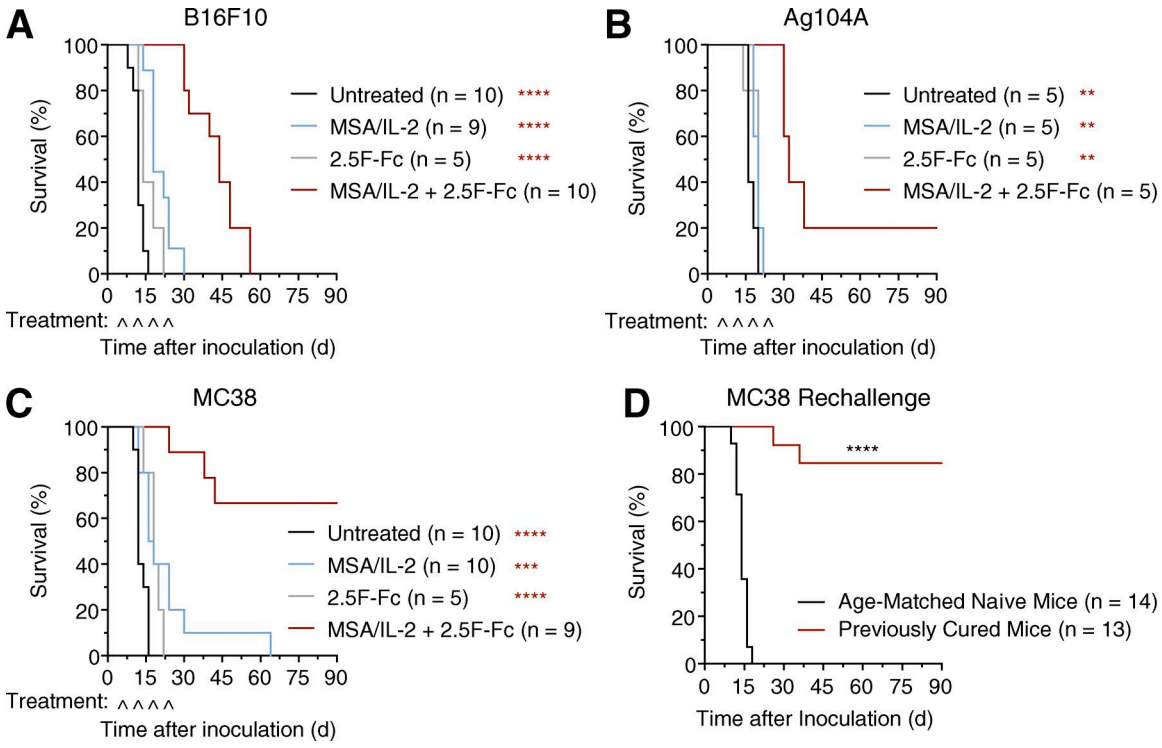

Figure 2. **2.5F-Fc combines with MSA/IL-2 to achieve synergistic antitumor efficacy in three syngeneic murine models of cancer and leads to protective immunity against tumor rechallenge in some mice.** (A–C) Survival curves demonstrating the synergistic efficacy of MSA/IL-2 + 2.5F-Fc. Syngeneic mice bearing 6 d B16F10 melanoma (A), Ag104A fibrosarcoma (B), or MC38 colon carcinoma tumors (C) were treated as indicated. **, $P < 0.01$; ***, $P < 0.001$; ****, $P < 0.0001$ versus the MSA/IL-2 + 2.5F-Fc–treated condition determined by a log-rank Mantel–Cox test. A and C represent data from two pooled independent experiments, and B represents a single experiment. (D) Survival curve demonstrating the growth of MC38 tumor rechallenge at a distal site in previously cured mice and age-matched naive controls without further treatment. Mice were rechallenged 15–20 wk after the initial tumor inoculation. ****, $P < 0.0001$ by a log-rank Mantel–Cox test comparing the two groups. D represents data from four pooled independent experiments.

the clinical history for IL-2 (Siegel and Puri, 1991; Schwartz et al., 2002). Importantly, even in the liver samples with the highest amounts of inflammation, apoptotic events were very rare and no foci of necrosis were observed. Therefore, whereas hepatocyte function may have been transiently impaired, they were not eliminated by treatment and ultimately recovered.

Vascular disruption and tumor endothelial targeting are irrelevant to the efficacy of MSA/IL-2 + 2.5F-Fc

Given that earlier clinical attempts focused on antagonizing integrins expressed in rapidly proliferating tumor vasculature (Strömblad and Cheresh, 1996; Desgrosellier and Cheresh, 2010; Weis and Cheresh, 2011a), we investigated the contribution of vascular targeting to our results by using a previously described mouse model to delete α_v and α_5 integrin genes from the endothelium of the mouse by tamoxifen-inducible Cre-lox–dependent recombination (Murphy et al., 2015). We confirmed a lack of 2.5F-Fc binding to aortic endothelial cells after tamoxifen administration in those mice containing Cre, but not those mice lacking the Cre gene (Fig. S3 A). After establishing the validity of the model with respect to 2.5F-Fc binding to endothelial cells, we tested for antitumor efficacy using MSA/IL-2 and 2.5F-Fc in MC38 tumors to determine if the efficacy of the therapy would be affected in the absence of endothelial targeting. Tumor growth was similar in mice with endothelial deletion of α_v and α_5 and tamoxifen-treated controls (Fig. 4 A and Fig. S3 B), recapitulating previous results that indicate no essential role for these integrins in the formation of tumor vasculature (Murphy et al., 2015). Upon treatment, no significant difference in antitumor responses was observed between the efficacy of the combination treatment in mice with or without conditional integrin gene deletions (Fig. 4 A and Fig. S3 B). Furthermore, no significant changes in vessel density were observed upon treatment (Fig. 4 B), indicating that endothelial targeting of 2.5F-Fc is not a necessary component of its therapeutic mechanism of action.

Integrin antagonism is not sufficient to drive efficacy in the absence of immune effector function

To determine the contribution of functional integrin antagonism in the absence of antibody effector functions, we introduced a D265A mutation into the Fc domain of 2.5F-Fc (2.5F-D265AFc), which has been described to abrogate

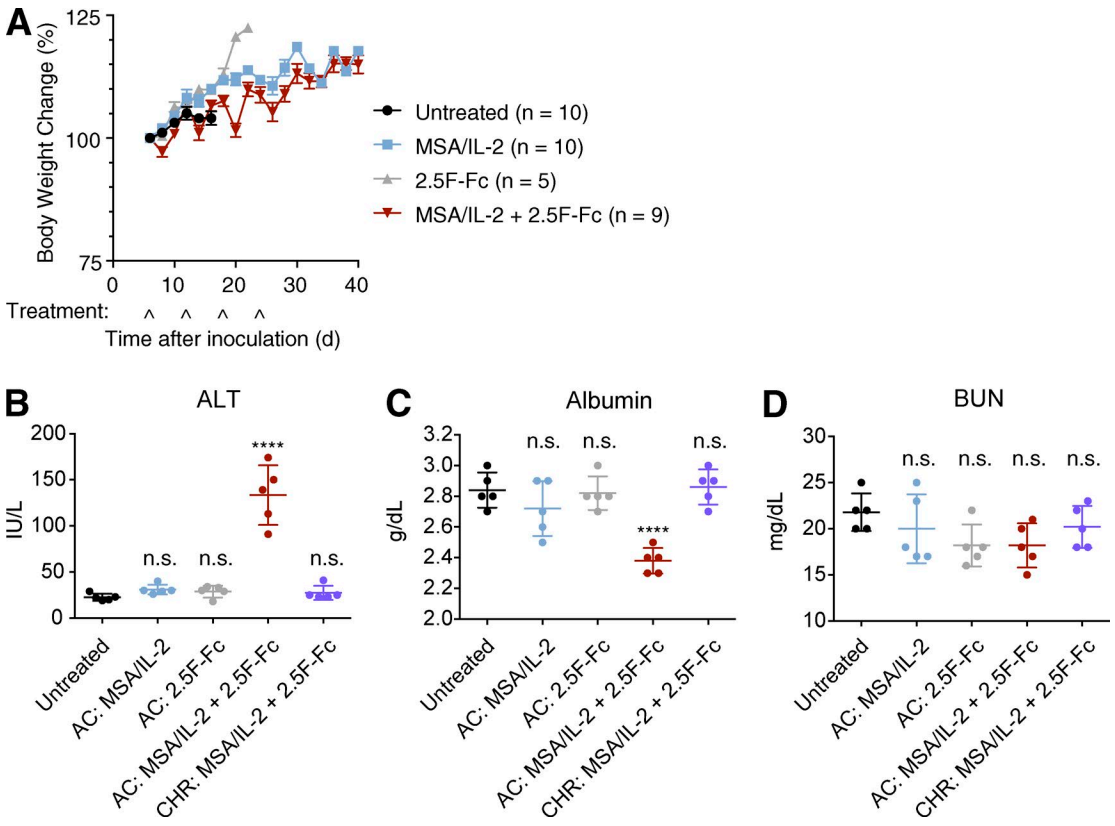

Figure 3. **MSA/IL-2 + 2.5F-Fc is well tolerated despite transient and reversible liver inflammation.** (A) Percent change in body weight of mice bearing MC38 tumors throughout the course of treatment as indicated. Percent change is calculated relative to body weight on the day of the first treatment, before treatment. Symbols and error bars represent means ± SEM. A represents data from two pooled independent experiments. (B–D) Serum analysis of alanine transaminase (ALT; B), albumin (C), and blood urea nitrogen (BUN; D) levels to assess liver (ALT/albumin) and kidney (BUN) function in mice receiving treatment. AC: Non–tumor-bearing mice were assayed 48 h after four cycles (treatment every 6 d) of the indicated treatment to assess acute treatment effects. CHR: Mice that have demonstrated protective immunity against MC38 tumors after treatment with MSA/IL-2 + 2.5F-Fc were assayed between 15 and 54 wk after the final treatment to assess chronic treatment effects. ****, $P < 0.0001$; n.s., not significant by one-way ANOVA with Dunnett's post-test for analyzing comparisons with the untreated group. Midlines and error bars represent means ± SD ($n = 5$). B–D represent data from a single experiment.

binding of FcγR and complement activation while retaining binding to the neonatal Fc receptor and preserving its pharmacokinetic profile (Shields et al., 2001; Baudino et al., 2008). When 2.5F-D265AFc was administered alongside MSA/IL-2, the previously observed efficacy was nullified in both the B16F10 and MC38 tumor models (Fig. 4 C and Fig. S3, C and D), closely resembling that of MSA/IL-2 administered as monotherapy (Fig. 2, A and C). Thus, integrin antagonism is insufficient for 2.5F-Fc therapy, and engagement of innate effectors is required for efficacy.

Cellular biodistribution assay reveals differential uptake of 2.5F-Fc and 2.5F-D265AFc by macrophages and DCs

Because there was a significant difference between 2.5F-Fc and the inactivated Fc variant, we examined the contribution of the 2.5F and Fc moieties to 2.5F-Fc's cellular-level tropism by determining the cellular biodistribution (Tzeng et al., 2015) of fluorescently labeled 2.5F-Fc and 2.5F-D265AFc in the tumor-draining lymph node 24 h after administration in MC38 tumor-bearing mice. Macrophages and DCs took up 2.5F-Fc significantly more than 2.5F-D265AFc, whereas negligible differences were observed between the two constructs in T cells, B cells, neutrophils, and NK cells (Fig. 5 A). FcγR-mediated uptake by macrophages and DCs therefore correlates with therapeutic efficacy. It is noteworthy that despite measurable 2.5F-D265AFc uptake, consistent with expression of these integrins on the surface of immune cells, 2.5F-mediated binding does not lead to significant depletion of neutrophils, lymphocytes, or monocytes after a full course of treatment (Fig. 5 B).

$CD8^+$ T cells, macrophages, and DCs are the key immune effectors in therapy with MSA/IL-2 and 2.5F-Fc

To establish the components of the immune system required for antitumor efficacy using MSA/IL-2 + 2.5F-Fc, we systematically depleted various immune effector cells using antibodies against their respective lineage markers in mice bearing MC38 tumors. Unsurprisingly, as they are critical for

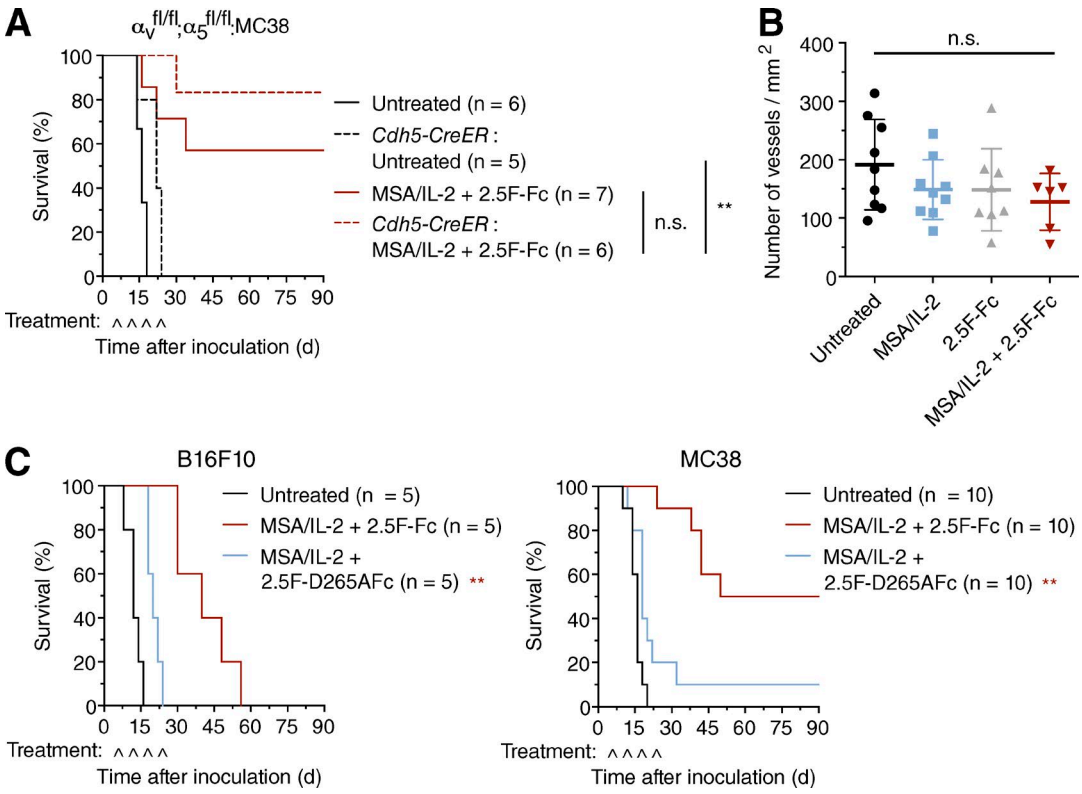

Figure 4. **Endothelial cell targeting and functional integrin antagonism by 2.5F-Fc are irrelevant for therapeutic efficacy.** (A) Survival curve demonstrating no difference in therapeutic efficacy of MSA/IL-2 + 2.5F-Fc in mice with or without α_v and α_5 integrin expression on endothelial cells and treated as indicated. Endothelial cell–specific and tamoxifen-inducible Cre-lox–mediated deletion of integrins was elicited by *Cdh5-CreER*. All mice received tamoxifen before tumor inoculation; mice without the *Cdh5-CreER* gene retain integrin expression and were included to account for potential tamoxifen-mediated effects. **, $P < 0.01$; n.s., not significant by a log-rank Mantel–Cox test, and all statistical comparisons were performed as indicated. A represents data from three pooled independent experiments. (B) Vessel density of frozen MC38 tumor sections after treatment. Vessels were identified using anti-CD31 antibody. n.s., not significant by one-way ANOVA. Midlines and error bars represent means ± SD (untreated and MSA/IL-2: $n = 9$; 2.5F-Fc: $n = 8$; MSA/IL-2 + 2.5F-Fc: $n = 6$). B represents data from two pooled independent experiments. (C) Survival curves exhibiting the difference in potency between 2.5F-Fc and 2.5F-D265AFc (lacking Fc-mediated effector function) on therapeutic efficacy in B16F10 melanoma and MC38 colon carcinoma tumors. **, $P < 0.01$ versus the MSA/IL-2 + 2.5F-Fc–treated condition determined by a log-rank Mantel–Cox test. C represents data from two pooled independent experiments (MC38) and a single experiment (B16F10).

most efficacious antitumor immune responses (Mellman et al., 2011), $CD8^+$ T cells were required for therapeutic efficacy (Fig. 6 A and Fig. S4 A). The absence of $CD4^+$ T cells did not substantially alter the therapeutic efficacy of the treatment in the short-term but did negatively impact the long-term survival of the mice (Fig. 6 A and Fig. S4 A). Though known to exert Fc-mediated effector function, NK cells, neutrophils, B cells, and the complement system were not individually important for therapeutic efficacy (Fig. 6, B and C; and Fig. S4 A). In fact, macrophages appeared to be the key innate effector, as administration of anti–CSF-1R antibody alongside MSA/IL-2 and 2.5F-Fc resulted in a significant decrease of long-term survivors (Fig. 6 B and Fig. S4 A). Furthermore, 24 h after the combination treatment, soluble factors in the tumor microenvironment associated with macrophage activation, MIP-1α, MIP-1β, and MIP-2 (Wolpe and Cerami, 1989; Maurer and von Stebut, 2004), were significantly increased relative to untreated and singly treated controls (Fig. 6 E). Finally, to probe the function of DCs in this system, we used mice lacking the gene for the Batf3 transcription factor (Batf3 KO), which do not have the ability to mature $CD8^+$ DCs and are thus deficient in cross-presentation (Hildner et al., 2008). Batf3 KO mice bearing 6 d tumors demonstrated significantly fewer responders to MSA/IL-2 and 2.5F-Fc treatment and lower overall survival when compared with wild-type mice (Fig. 6 D and Fig. S4 B). Collectively, these results suggest a critical role for $CD8^+$ T cells, macrophages, and DCs in the therapeutic efficacy mediated by MSA/IL-2 and 2.5F-Fc, concordant with the results of the cellular biodistribution assay (Fig. 5 A).

Addition of an anti–PD-1 checkpoint blockade antibody to MSA/IL-2 and 2.5F-Fc enhances antibody responses and results in cures

Because the mechanisms of action of checkpoint blockade and our combination immunotherapy are likely distinct and

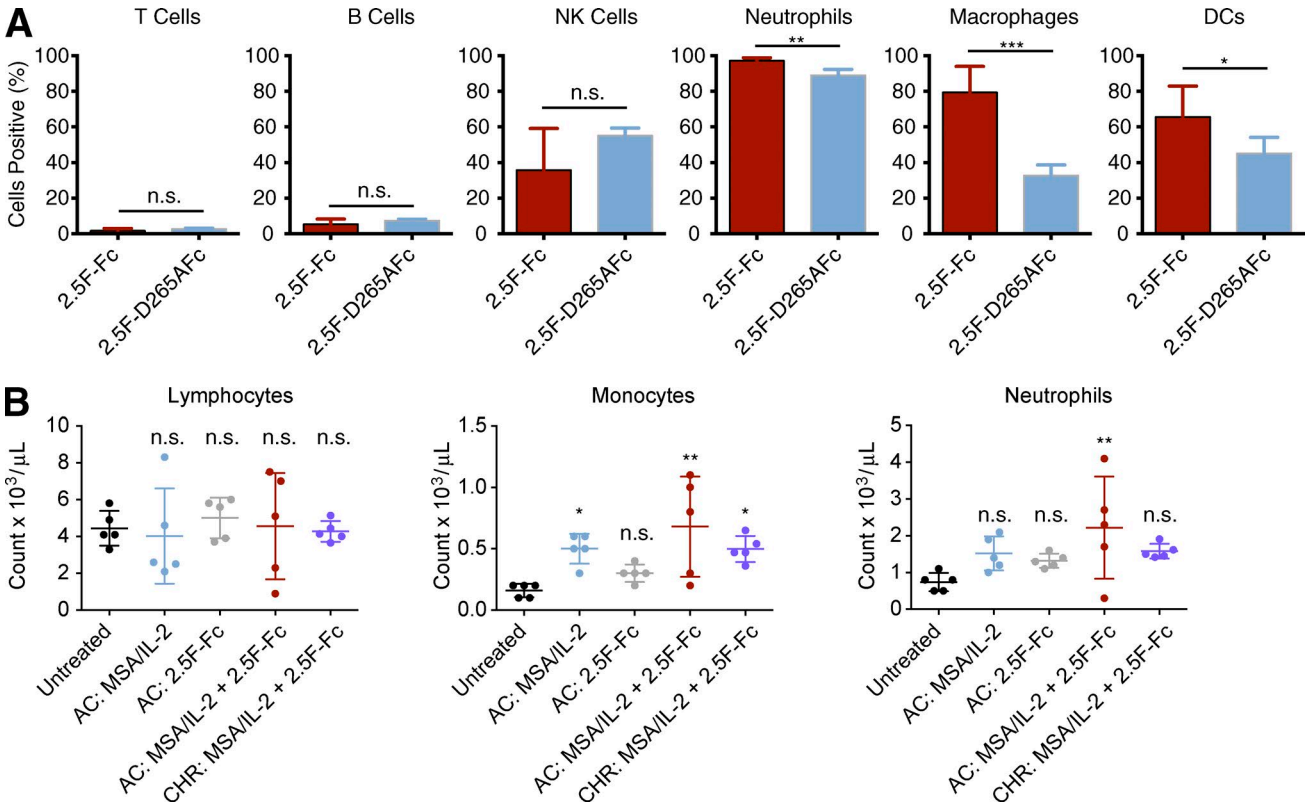

Figure 5. **2.5F-Fc associates with immune cells through both integrin and FcγR-mediated interactions without deleterious effects on immune cell populations.** (A) Cellular biodistribution assay determining the percentage of indicated immune cells interacting with 2.5F-Fc or 2.5F-D265AFc in the tumor draining lymph node. Bars and error bars represent means ± SD. For T, B, and NK cells, $n = 4$ for 2.5F-Fc and $n = 5$ for 2.5F-D265AFc. For others, $n = 5$ for all samples. *, $P < 0.05$; **, $P < 0.01$; ***, $P < 0.001$; n.s., not significant by two-tailed Student's t test. A represents data from a single experiment. (B) CBC analysis of lymphocytes, monocytes, and neutrophils in mice receiving treatment. AC: Non–tumor-bearing mice were assayed 48 h after four cycles (treatment every 6 d) of the indicated treatment to assess acute treatment effects. CHR: Mice that have demonstrated protective immunity against MC38 tumors after treatment with MSA/IL-2 + 2.5F-Fc were assayed between 15 and 54 wk after the final treatment to assess chronic treatment effects. *, $P < 0.05$; **, $P < 0.01$; n.s., not significant by one-way ANOVA with Dunnett's post-test for analyzing comparisons to the untreated group. Midlines and error bars represent means ± SD ($n = 5$). B represents data from a single experiment.

nonoverlapping, we explored the potential of using an anti–PD-1 antibody alongside MSA/IL-2 and 2.5F-Fc. When treated with this triple combination, 15 out of 17 mice bearing MC38 tumors survived beyond 90 d after tumor inoculation and achieved cures (Fig. 7 and Fig. S5). Note that although neither of the singly treated or doubly treated combinations performed as well as the triple combination, both MSA/IL-2 and 2.5F-Fc each significantly increased anti–PD-1 monotherapy effectiveness, presumably by induction of the $CD8^+$ T cell response shown to be required for efficacy.

DISCUSSION

Although all prior integrin-targeted therapies have failed in clinical trials, we demonstrate here that these integrins provide an excellent target for therapeutic antibody Fc effector functions that synergize with IL-2 cytokine therapy to achieve robust antitumor responses without significant toxicity. Previous antibodies targeting either $\alpha_v\beta_3$ (Mulgrew et al., 2006) or $\alpha_5\beta_1$ (Li et al., 2010) integrin with activating Fc isotypes lacked the broad cross-reactivity of 2.5F-Fc and were not explored in the context of combination immunotherapy.

Macrophages appear to be the primary innate cellular effector (Figs. 5 A and 6 B and Fig. S4 A). Counterintuitively, anti–CSF-1R antibodies such as the one used in this study to deplete tumor-associated macrophages are themselves a cancer immunotherapeutic currently being clinically evaluated (MacDonald et al., 2010; Ries et al., 2014; Ruffell and Coussens, 2015). In fact, as a monotherapy, anti–CSF-1R therapy modestly inhibits the growth of MC38 tumors by clearing these immunosuppressive tumor-associated macrophages (Ries et al., 2014). However, the combination therapy described in this work appears to direct macrophages against the tumor through antibody Fc-mediated effectors and therefore would suffer from the loss of a key effector population.

In this study, although we show that targeting the vasculature is not a source of therapeutic efficacy, expression of $\alpha_v\beta_3$ on immune cells such as macrophages may complicate interpretation. For example, $\alpha_v\beta_3$ on macrophages has been

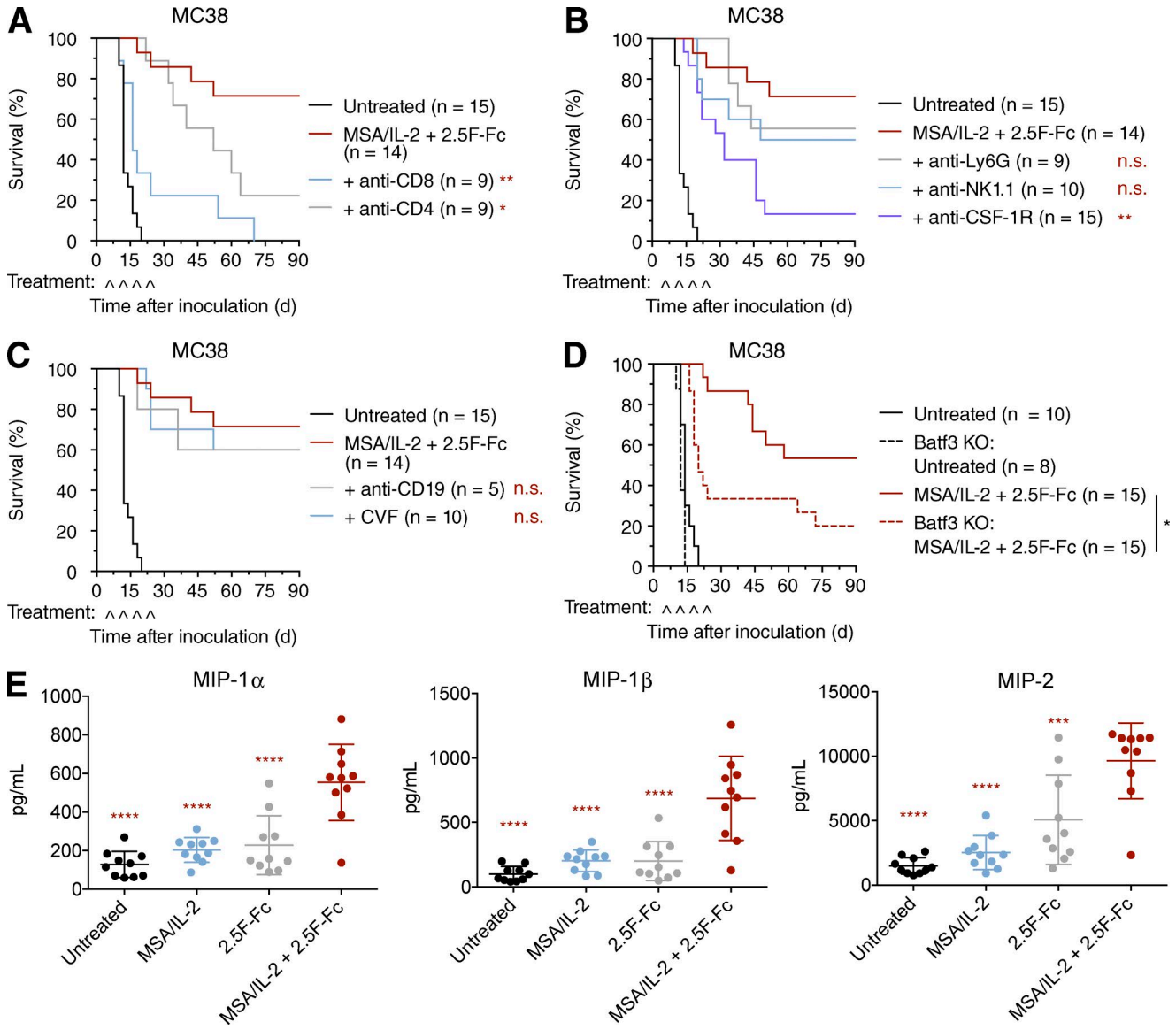

Figure 6. **CD8⁺ and CD4⁺ T cells, macrophages, and DCs are essential to therapeutic efficacy in MC38 colon carcinoma tumors.** (A–C) Survival curves demonstrating the significance of antibody-mediated or cobra venom factor (CVF)–mediated depletion of T cells (A), innate immune effectors (B), and B cells and complement system (C) on therapeutic efficacy in MC38 tumors in the context of MSA/IL-2 + 2.5F-Fc therapy. *, $P < 0.05$; **, $P < 0.01$; n.s., not significant versus the MSA/IL-2 + 2.5F-Fc–treated condition without depletion antibodies determined by a log-rank Mantel–Cox test. A–C represent data from three pooled independent experiments. (D) Survival curve demonstrating therapeutic efficacy in mice missing the Batf3 transcription factor, which is critical for DC-mediated cross-presentation. *, $P < 0.05$ by a log-rank Mantel–Cox test; statistical comparisons were performed as indicated. D represents data from two pooled independent experiments. (E) Intratumoral levels of the indicated cytokines after treatment in mice bearing 6 d MC38 tumors. Samples were normalized by total protein content before analysis to account for differences in tumor mass. ***, $P < 0.001$; ****, $P < 0.0001$ by one-way ANOVA with Dunnett's post-test for analyzing comparisons with the MSA/IL-2 + 2.5F-Fc–treated group. Midlines and error bars represent means ± SD ($n = 10$). E represents data from a single experiment.

shown to interact with MFG-E8 on tumor cells in such a way as to inhibit inflammatory antigen presentation (Jinushi et al., 2009). However, simple antagonism of this pathway cannot account for the observed efficacy because Fc-mediated effector functions are required. Furthermore, the development of complete tumor responses with subsequent immunological memory indicates that tumor antigen has been presented to CD8⁺ T cells in an activating fashion (Mellman et al., 2011).

Given the demonstration here of significant preclinical efficacy against three syngeneic murine models of cancer, including the development of cures and immunological memory, the combination of IL-2 cytokine therapy and 2.5F-Fc

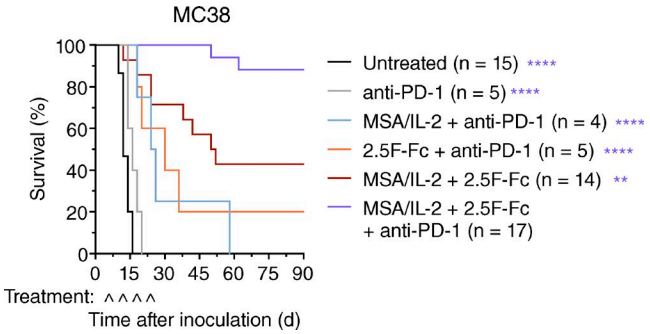

Figure 7. **An anti–PD-1 antibody combined with MSA/IL-2 and 2.5F-Fc results in significantly improved antitumor efficacy relative to single or double treatments in MC38 colon carcinoma tumors.** Survival curve demonstrating therapeutic efficacy of combinations of MSA/IL-2, 2.5F-Fc, and anti-PD-1 in mice bearing 6 d MC38 tumors. **, $P < 0.01$; ****, $P < 0.0001$ versus the MSA/IL-2 + 2.5F-Fc + anti-PD-1–treated condition determined by a log-rank Mantel–Cox test. Data shown are from three pooled independent experiments.

has potential for clinical translation. As 2.5F is cross-reactive against both murine and human integrins, the transition from mouse to human involves a simple isotype switch of murine IgG2a to human IgG1 Fc. Furthermore, administration of human IL-2 is an approved treatment for metastatic melanoma and renal cancers (Rosenberg, 2012), precluding the need for the approval of two novel agents. Finally, the clinical activity of immune checkpoint blockade and its status as the flagship of immuno-oncology make it probable that future immunotherapeutics will either be used (a) in conjunction with an anti–PD-1 antibody or (b) to treat patients whose disease has progressed while undergoing anti–PD-1 therapy. The demonstration here of synergistic effects from combining 2.5F-Fc and IL-2 therapy with an anti–PD-1 antibody indicate a favorable pathway for clinical development in any of the growing number of indications with anti–PD-1 antibodies as standard of care.

MATERIALS AND METHODS

Vector construction and amplification

The DNA sequences encoding 2.5F as previously described (Kimura et al., 2009a,b) and the C57BL/6 allele of the mIgG2a Fc domain (also known as mIgG2c) were cloned into the gWIZ vector (Genlantis) to form gWIZ-2.5F-Fc. The D265A point mutation as previously described (Shields et al., 2001; Baudino et al., 2008) was introduced into the mIgG2a Fc domain in gWIZ-2.5F-Fc to form gWIZ-2.5F-D265AFc. Construction of gWIZ-MSA/IL-2, which is the gWIZ vector containing the MSA/IL-2 gene along with a 6xHis tag, was described previously (Zhu et al., 2015). All plasmid DNA was transformed and amplified in Stellar Competent Cells (Takara Bio Inc.) and subsequently purified using the NucleoBond Xtra Maxi EF endotoxin-free maxiprep kit (Takara Bio Inc.).

Protein production

MSA/IL-2, 2.5F-Fc, and 2.5F-D265AFc were produced using the Freestyle 293-F (HEK) expression system (Thermo Fisher Scientific). Cells were cultured in Freestyle 293 media (Thermo Fisher Scientific) and transfected with gWIZ-MSA/IL-2, gWIZ-2.5F-Fc, or gWIZ-2.5F-D265AFc using polyethylenimine (Polysciences) as the transfection reagent and OptiPro serum-free medium (Thermo Fisher Scientific) as the transfection medium. MSA/IL-2 was purified using TALON Metal Affinity Resin (Takara Bio Inc.) followed by size exclusion chromatography using a HiLoad 16/600 Superdex 200 pg column on the ÄKTAFPLC system (GE Healthcare), as described previously (Zhu et al., 2015). 2.5F-Fc and 2.5F-D265AFc were purified using rProtein A Sepharose Fast Flow resin (GE Healthcare). All proteins were buffer exchanged into 1× PBS and passed through a 0.2-µm filter (Pall). All columns used for purification were pretreated with 0.2M or 1M NaOH to remove endotoxins and all proteins were confirmed to contain minimal levels of endotoxin (< 0.1 EU per injection) using the endpoint chromogenic LAL assay (Lonza).

To assess purity of 2.5F-Fc and 2.5F-D265A, SDS-PAGE using a Novex 4–12% Bis-Tris gel (Thermo Fisher Scientific) was performed using standard methods. Furthermore, purified proteins were analyzed using a Superdex 200 Increase 10/300 GL column on the ÄKTAFPLC system (GE Healthcare). For cellular biodistribution or binding studies 2.5F-Fc and 2.5F-D265A proteins were labeled with an amine-reactive Alexa Fluor 647 dye (AF647; Thermo Fisher Scientific) using the manufacturer's protocols.

ELISA binding assay

All RGD-binding integrins available for purchase (R&D Systems) were immobilized on NUNC 96-well MaxiSorp plates (eBioscience) at a concentration of 0.5 µg/ml in 1x PBS overnight at 4°C. Plates were washed in between steps with integrin-binding saline with Tween-20 (IBST), similar to one previously described (Kimura et al., 2009a) containing Tween-20 and divalent cations for integrin binding: 25 mM Tris, 150 mM NaCl, 2 mM $CaCl_2$, 1 mM $MgCl_2$, 1 mM $MnCl_2$, 0.05% wt/vol Tween-20. The wells were blocked with IBST + 1% wt/vol bovine serum albumin (IBSTA) for 1 h at room temperature and incubated with various concentrations of 2.5F-Fc in IBSTA for 2 h at room temperature, followed by a 1:1,000 dilution of goat anti–mouse horseradish peroxidase–conjugated secondary antibody (R&D Systems) in IBSTA for 1 h at room temperature. 1-Step Ultra TMB-ELISA Substrate Solution (Thermo Fisher Scientific) was added for 5 min followed by 2M H_2SO_4 to stop the chromogenic reaction. Absorbance was measured using a Tecan Infinite M1000 plate reader at 450 nm and background correction at 570 nm was subtracted from each sample. A nonlinear binding curve was fit to the data from three independent experiments using GraphPad Prism 6.

Cell culture

B16F10 cells (ATCC) were cultured in DMEM (ATCC) with 10% FBS (Thermo Fisher Scientific). Ag104A cells (Ward et al., 1989) were a gift from H. Schreiber (University of Chicago, Chicago, IL), and MC38 cells were a gift from J. Schlom (National Cancer Institute, Bethesda, MD); both cell lines were also cultured in DMEM with 10% FBS. All cell lines were subjected to IMPACT I PCR testing (IDEXX Laboratories) to confirm a lack of murine pathogens.

Mice

For wild-type mice, female C57BL/6N (syngeneic with B16F10 and MC38) or C3H/HeN (syngeneic with Ag104A) mice were purchased from Taconic and were between 6 and 10 wk of age at the time of tumor induction. Generation of $\alpha_v^{fl/fl}$; $\alpha_5^{fl/fl}$ and *Cdh5-CreER*; $\alpha_v^{fl/fl}$; $\alpha_5^{fl/fl}$ mice was performed as previously described (Murphy et al., 2015). Batf3 KO (B6.129S(C)-*Batf3*^{tm1Kmm}/J) mice used in this study were expanded from a breeding pair purchased from The Jackson Laboratory.

Tumor inoculation and treatment

10^6 B16F10, Ag104A, or MC38 tumor cells were injected subcutaneously into the right flanks of syngeneic wild-type mice or genetically modified mice, as indicated. For rechallenge experiments, previously bearing MC38 tumors that achieved a complete response, along with age-matched naive control mice, were rechallenged in the left flank with 10^6 MC38 tumor cells 15–20 wk after the initial tumor inoculation. Tumor measurements were taken every 2 d starting on day 6 after tumor inoculation using calipers, and tumor area was calculated using length × width. Mouse weights were also recorded every 2 d starting on day 6 after tumor inoculation.

For treatment, i.p. injections of 30 µg MSA/IL-2, 500 µg 2.5F-Fc, 500 µg 2.5F-D265AFc, and/or 200 µg anti–PD-1 (clone RMP1-14; Bio X Cell) were done on days 6, 12, 18, and 24 after tumor inoculation for a total of four treatments. For antibody-mediated depletions, anti-CD8α (clone 2.43), anti-CD4 (clone GK1.5), anti-NK1.1 (clone PK136), anti-Ly6G (clone 1A8), and anti-CD19 (clone 1D3) were administered at a dose of 400 µg every 4 d starting on day 4 after tumor inoculation for a total of six doses, and anti–CSF-1R (clone AFS98) was administered at a dose of 300 µg every 2 d starting on day 4 after tumor inoculation for a total of eleven doses. All depletion antibodies were dosed i.p. and purchased from BioXCell. To deplete complement, cobra venom factor from *Naja naja kouthia* (EMD Millipore) was administered i.p. at a dose of 30 µg every 6 d starting on day 5 after tumor inoculation for a total of four doses. Justification and validation for depletion schedules and doses is described previously (Zhu et al., 2015).

For experiments using $\alpha_v^{fl/fl}$; $\alpha_5^{fl/fl}$ and *Cdh5-CreER*; $\alpha_v^{fl/fl}$; $\alpha_5^{fl/fl}$ mice, tamoxifen was administered i.p. to mice 7, 5, and 3 d before tumor inoculation at a dose of 1 mg as previously described (Murphy et al., 2015).

Complete blood count (CBC), serum, and histopathological analysis

For acute (AC) analysis of the effect of treatment on serum markers and CBC, healthy (non–tumor-bearing) C57BL/6N mice were given 30 µg MSA/IL-2 + 500 µg 2.5F-Fc by i.p. injection every 6 d for a total of four treatments. 2 d after the fourth and final treatment, blood was collected by retro-orbital bleeding with heparin-coated capillary tubes (VWR) into K3 EDTA coated tubes (Sarstedt) for whole-blood analysis and serum separation tubes (BD) for serum analysis. For chronic analysis, mice that were previously cured of MC38 tumors and survived MC38 tumor rechallenge were used in the same fashion between 15 and 54 wk after the fourth and final treatment. Whole blood was analyzed using the Hemavet 950 FS (Drew Scientific) and CBC with auto differential was acquired. Serum was analyzed using the Chem 11 Panel (IDEXX Laboratories). The liver, lungs, kidneys, and spleen were removed from each mouse for histopathological analysis. These organs were fixed in 10% neutral buffered formalin (Sigma-Aldrich), paraffin embedded, sectioned, and stained with hematoxylin and eosin. Blinded analysis of the tissue sections was performed and scored based on immune infiltrate.

Aortic endothelial cell–binding experiments in Cdh5-CreER; $\alpha_v^{fl/fl}$; $\alpha_5^{fl/fl}$ mice

To determine whether 2.5F-Fc could still bind to the vasculature of $\alpha_v^{fl/fl}$; $\alpha_5^{fl/fl}$ or *Cdh5-CreER*; $\alpha_v^{fl/fl}$; $\alpha_5^{fl/fl}$ mice after tamoxifen administration, aortic endothelial cells were analyzed for 2.5F-Fc binding using flow cytometry. $\alpha_v^{fl/fl}$; $\alpha_5^{fl/fl}$ or *Cdh5-CreER*; $\alpha_v^{fl/fl}$; $\alpha_5^{fl/fl}$ mice were given 1 mg tamoxifen every 2 d for a total of three treatments. The aorta was harvested, filled with a 2% collagenase II solution, and allowed to incubate for 1 h at 37°C. Cells in the aorta were then flushed out and cultured for 1 wk before being stained with anti–CD31-BV421 (clone MEC13.3; BD) and AF647-labeled 2.5F-Fc in buffers with and without Ca^{2+}, Mg^{2+}, and Mn^{2+}, as integrin binding to the RGD motif requires these divalent cations (Hynes, 1992). Binding of endothelial cells ($CD31^+$ cells) to AF647-labeled 2.5F-Fc was analyzed by an LSR-Fortessa flow cytometer (BD).

Vessel density of MC38 tumors

C57BL/6N mice were inoculated with 10^6 MC38 cells, and tumors were allowed to establish for 6 d. 30 µg MSA/IL-2 and/or 500 µg 2.5F-Fc were administered i.p. starting on days 6 and 12 after tumor inoculation. On day 15 after tumor inoculation, tumors were excised and snap-frozen in Tissue-Tek OCT compound (Sakura) and sectioned onto slides. These slides were stained using rat anti-CD31 (BD clone MEC13.3) in combination with the anti–rat Ig HRP detection kit (BD) according to the manufacturer's protocol. Slides were then imaged using a slide scanner (Leica Biosystems).

Vessels in tumors were counted using a program written in Java. In brief, a color-based filter was used to identify pixels with RGB values that matched those of the stained

vessels. The images were then converted to greyscale, so as to reduce the RGB image (where each pixel has three values) to a simpler format (where each pixel has one value). The images were then polarized to yield a black-and-white duplicate, where any pixel with a value over a certain threshold was colored white and other pixels were colored black. Finally, all pixels without valid "neighbors" (i.e., noise) were eliminated, leaving isolated vessels, which were quantified. This image analysis was performed on at least three distinct regions of each tumor sample that was nonnecrotic, and each point on the graph represents the mean number of vessels/tumor area.

Cellular biodistribution of 2.5F-Fc and 2.5F-D265AFc

To determine the distribution of 2.5F-Fc and 2.5F-D265AFc across different immune cells, the cellular biodistribution assay was performed as previously described (Tzeng et al., 2015). C57BL/6N mice were inoculated with 10^6 MC38 cells, and tumors were allowed to establish for 6 d. Mice were treated i.p. with 30 µg MSA/IL-2, 500 µg MSA/IL-2 + AF647-labeled 2.5F-Fc, or 500 µg MSA/IL-2 + AF647-labeled 2.5F-D265AFc. 24 h later, mice were euthanized, and the tumor-draining lymph nodes were dissected and mechanically dissociated. The resulting cell suspensions were stained with Zombie Aqua Live/Dead stain (BioLegend) and incubated with Trustain FcX (Fc blocking reagent; BioLegend) before staining with either (1) anti–CD3e-BUV395 (BD clone 145-2C11), anti–CD19-PE (clone 6D5; BioLegend), and anti–NK1.1-Alexa Fluor 488 (clone PK136; BioLegend) or (2) anti–CD11b-BUV395 (clone M1/70; BD), anti-CD11c-PE (clone N418; BioLegend), anti-Ly6G-FITC (clone 1A8; BioLegend), anti–F4/80-BV711 (clone BM8; BioLegend), anti-CD3e-PerCP/Cy5.5 (clone 145-2C11; BioLegend), anti–CD19-PerCP/Cy5.5 (clone 6D5; BioLegend), and anti–NK1.1-PerCP/Cy5.5 (clone PK136; BioLegend). Cell suspensions were treated with Fixation Buffer (eBioscience) and then analyzed using an LSR-Fortessa flow cytometer.

Data analysis was performed using FlowJo v10. Only singlet live cells were included in the analysis. Cell types were defined as follows: T cells were $CD3e^+$, $NK1.1^-$, $CD19^-$; B-cells were $CD19^+$, $NK1.1^-$, $CD3e^-$; NK-cells were $NK1.1^+$, $CD19^-$, $CD3e^-$; neutrophils were $CD11b^+$, $Ly6G^+$, $CD3e^-$, $CD19^-$, $NK1.1^-$; macrophages were $CD11b^+$, $F4/80^+$, $Ly6G^-$, $CD3e^-$, $CD19^-$, $NK1.1^-$; and DCs were $CD11c^+$, $F4/80^-$, $Ly6G^-$, $CD3e^-$, $CD19^-$, $NK1.1^-$. Percentage of cells positive was defined as the percentage of cells having an AF647 intensity signal higher than a background gate established using MSA/IL-2 only–treated controls (where <1% cells are positive). The same gates were used for all samples.

Intratumoral cytokine analysis

C57BL/6N mice were inoculated with 10^6 MC38 cells, and tumors were allowed to establish for 6 d. Mice were treated i.p. with 30 µg MSA/IL-2 and/or 500 µg 2.5F-Fc as indicated on day 6 after tumor inoculation. All mice were euthanized 24 h later, and tumors were homogenized in tubes containing zirconium beads (KSE Scientific) using a Mini-Beadbeater-16 (Biospec Products) in buffer containing "cOmplete" Protease Inhibitor Cocktail (Roche). To account for differences in tumor size, protein concentrations for all samples were normalized using the bicinchoninic acid assay (Thermo Fisher Scientific) and were snap-frozen in liquid nitrogen. Samples were evaluated in duplicate using the Mouse Cytokine/Chemokine Array 31-Plex (Eve Technologies).

Experimental design

To evaluate the prospect of integrin-targeted immunotherapy, we used syngeneic subcutaneous flank tumors in mice. Before the initiation of treatment (or antibody depletion), animals were placed into treatment groups such that each group had mean tumor areas with as little intergroup variation as possible. The primary endpoint for survival analysis was preselected to be a tumor burden of 100 mm^2, and before the initiation of studies, it was established that all mice requiring euthanasia or found dead for reasons other than tumor burden (e.g., ulcerative dermatitis or malocclusion) would be excluded from analysis.

Sample sizes and replicates were chosen based on prior experience, and sample sizes are indicated in the figure legends. Figs. 1 (B and C), 4 A, 6 (A–C), and 7 and Figs. S3 B, S4 A, and S5 represent data from three pooled independent experiments. Figs. 2 (A and C), 3 A, 4 (B and C; MC38), and 6 D and Figs. S1 (A and C), S3 D, and S4 B represent data from two pooled independent experiments. Fig. 2 D and Fig. S1 D represent data from four pooled independent experiments. All other figures are the result of one experiment. Data collection was not blinded, with the exception of histopathological scoring.

Statistics

All statistical analyses were performed using GraphPad Prism 6.0. The identity of the statistical test performed, definitions of central tendency and dispersion, and p-values and *n* values are stated in the figure legends. Comparisons of survival curves were performed using a log-rank Mantel-Cox test to compare two treatment groups. Comparisons of blood chemistry, CBC, vessel density, and intratumoral cytokine data were performed using a one-way ANOVA, with Dunnett's post-test for analyzing comparisons to a specific group. Cellular biodistribution data were compared using a Student's *t* test, which assumed normally distributed data and was two tailed. For all tests, the threshold for significance was $P < 0.05$.

Study approval

All animal work was conducted under the approval of the Massachusetts Institute of Technology Division of Comparative Medicine in accordance with federal, state, and local guidelines.

Online supplemental material

The supplementary information contains plots of tumor area as a function of time for each mouse represented in the sur-

vival curves from the main text, histopathology scoring, and validation of the *Cdh5-CreER*; $\alpha_v^{fl/fl}$; $\alpha_5^{fl/fl}$. Fig. S1 shows that 2.5F-Fc combines with MSA/IL-2 to achieve synergistic antitumor efficacy in three syngeneic mouse models of cancer and leads to protective immunity against tumor rechallenge in some mice. Fig. S2 shows the presence of inflammation as a result of treatment with MSA/IL-2 + 2.5F-Fc occurs primarily in the liver and lung, is not accompanied by foci of necrosis or apoptosis, and is predominantly mediated by IL-2. Fig. S3 shows that endothelial cell targeting and functional integrin antagonism by 2.5F-Fc are irrelevant for therapeutic efficacy. Fig. S4 shows that $CD8^+$ and $CD4^+$ T cells, macrophages, and DCs are essential to therapeutic efficacy in MC38 colon carcinoma tumors. Fig. S5 shows that anti–PD-1 antibody combined with MSA/IL-2 and 2.5F-Fc results in significantly improved antitumor efficacy relative to single or double treatments in MC38 colon carcinoma tumors.

ACKNOWLEDGMENTS

We thank Dr. Roderick Bronson for his assistance with blinded histopathological analysis, Ellen Buckley Jordan and Carolyn Madden for their assistance with CBC analysis, and the Koch Institute Swanson Biotechnology Center staff for their assistance with flow cytometry, histology, and imaging.

This work was supported by National Institutes of Health (NIH) grant CA174795, a Stanford Wallace H. Coulter Translational Partnership Award, NIH grant U54CA163109, and the Howard Hughes Medical Institute, of which R.O. Hynes is an Investigator. B.H. Kwan, E.F. Zhu, and A. Tzeng were supported by a National Science Foundation graduate fellowship. E.F. Zhu and N.K. Mehta were supported by the NIH/National Institute of General Medical Sciences Biotechnology Training Program. A. Tzeng was supported by a Siebel Scholarship. P.A. Murphy was supported by NIH grant K99HL125727. A. Angelini was supported by Swiss National Science Foundation Fellowship for Advanced Researcher PP00P3_123524/1 and a Ludwig Cancer Research Center Postdoctoral Fellowship.

Patent applications covering the therapeutic strategy described in this manuscript have been filed on behalf of Stanford and the Massachusetts Institute of Technology. A company (Nodus Therapeutics) has been founded by J.R. Cochran and K.D. Wittrup with the goal of translating this therapeutic strategy to the clinic. The authors declare no additional competing financial interests.

Author contributions: B.H. Kwan and K.D. Wittrup designed research studies. B.H. Kwan, E.F. Zhu, A. Tzeng, H.R. Sugito, A.A. Eltahir, B. Ma, M.K. Delaney, P.A. Murphy, M.J. Kauke, A. Angelini, N. Momin, and A.A. Maragh conducted experiments and acquired data. P.A. Murphy, N.K. Mehta., R.O. Hynes, G. Dranoff, and J.R. Cochran provided important reagents and advice. B.H. Kwan and K.D. Wittrup analyzed data and wrote the manuscript.

Submitted: 3 June 2016
Revised: 25 September 2016
Accepted: 23 March 2017

REFERENCES

Baudino, L., Y. Shinohara, F. Nimmerjahn, J. Furukawa, M. Nakata, E. Martínez-Soria, F. Petry, J.V. Ravetch, S. Nishimura, and S. Izui. 2008. Crucial role of aspartic acid at position 265 in the CH2 domain for murine IgG2a and IgG2b Fc-associated effector functions. *J. Immunol.* 181:6664–6669. http://dx.doi.org/10.4049/jimmunol.181.9.6664

Desgrosellier, J.S., and D.A. Cheresh. 2010. Integrins in cancer: biological implications and therapeutic opportunities. *Nat. Rev. Cancer.* 10:9–22. http://dx.doi.org/10.1038/nrc2748

Gajewski, T.F., S.-R. Woo, Y. Zha, R. Spaapen, Y. Zheng, L. Corrales, and S. Spranger. 2013. Cancer immunotherapy strategies based on overcoming barriers within the tumor microenvironment. *Curr. Opin. Immunol.* 25:268–276. http://dx.doi.org/10.1016/j.coi.2013.02.009

Goodman, S.L., and M. Picard. 2012. Integrins as therapeutic targets. *Trends Pharmacol. Sci.* 33:405–412. http://dx.doi.org/10.1016/j.tips.2012.04.002

Heidenreich, A., S.K. Rawal, K. Szkarlat, N. Bogdanova, L. Dirix, A. Stenzl, M. Welslau, G. Wang, F. Dawkins, C.J. de Boer, and D. Schrijvers. 2013. A randomized, double-blind, multicenter, phase 2 study of a human monoclonal antibody to human αv integrins (intetumumab) in combination with docetaxel and prednisone for the first-line treatment of patients with metastatic castration-resistant prostate cancer. *Ann. Oncol.* 24:329–336. http://dx.doi.org/10.1093/annonc/mds505

Hersey, P., J. Sosman, S. O'Day, J. Richards, A. Bedikian, R. Gonzalez, W. Sharfman, R. Weber, T. Logan, M. Buzoianu, et al. Etaracizumab Melanoma Study Group. 2010. A randomized phase 2 study of etaracizumab, a monoclonal antibody against integrin $\alpha_v\beta_3$, ± dacarbazine in patients with stage IV metastatic melanoma. *Cancer.* 116:1526–1534. http://dx.doi.org/10.1002/cncr.24821

Hildner, K., B.T. Edelson, W.E. Purtha, M. Diamond, H. Matsushita, M. Kohyama, B. Calderon, B.U. Schraml, E.R. Unanue, M.S. Diamond, et al. 2008. *Batf3* deficiency reveals a critical role for $CD8\alpha^+$ dendritic cells in cytotoxic T cell immunity. *Science.* 322:1097–1100. http://dx.doi.org/10.1126/science.1164206

Hood, J.D., and D.A. Cheresh. 2002. Role of integrins in cell invasion and migration. *Nat. Rev. Cancer.* 2:91–100. http://dx.doi.org/10.1038/nrc727

Hynes, R.O. 1992. Integrins: versatility, modulation, and signaling in cell adhesion. *Cell.* 69:11–25. http://dx.doi.org/10.1016/0092-8674(92)90115-S

Hynes, R.O. 2002. Integrins: bidirectional, allosteric signaling machines. *Cell.* 110:673–687. http://dx.doi.org/10.1016/S0092-8674(02)00971-6

Jinushi, M., M. Sato, A. Kanamoto, A. Itoh, S. Nagai, S. Koyasu, G. Dranoff, and H. Tahara. 2009. Milk fat globule epidermal growth factor-8 blockade triggers tumor destruction through coordinated cell-autonomous and immune-mediated mechanisms. *J. Exp. Med.* 206:1317–1326. http://dx.doi.org/10.1084/jem.20082614

Kimura, R.H., Z. Cheng, S.S. Gambhir, and J.R. Cochran. 2009a. Engineered knottin peptides: A new class of agents for imaging integrin expression in living subjects. *Cancer Res.* 69:2435–2442. http://dx.doi.org/10.1158/0008-5472.CAN-08-2495

Kimura, R.H., A.M. Levin, F.V. Cochran, and J.R. Cochran. 2009b. Engineered cystine knot peptides that bind αvβ3, αvβ5, and α5β1 integrins with low-nanomolar affinity. *Proteins.* 77:359–369. http://dx.doi.org/10.1002/prot.22441

Li, G., L. Zhang, E. Chen, J. Wang, X. Jiang, J.H. Chen, G. Wickman, K. Amundson, S. Bergqvist, J. Zobel, et al. 2010. Dual functional monoclonal antibody PF-04605412 targets integrin α5β1 and elicits potent antibody-dependent cellular cytotoxicity. *Cancer Res.* 70:10243–10254. http://dx.doi.org/10.1158/0008-5472.CAN-10-1996

MacDonald, K.P., J.S. Palmer, S. Cronau, E. Seppanen, S. Olver, N.C. Raffelt, R. Kuns, A.R. Pettit, A. Clouston, B. Wainwright, et al. 2010. An antibody against the colony-stimulating factor 1 receptor depletes the resident subset of monocytes and tissue- and tumor-associated macrophages but does not inhibit inflammation. *Blood.* 116:3955–3963. http://dx.doi.org/10.1182/blood-2010-02-266296

Maurer, M., and E. von Stebut. 2004. Macrophage inflammatory protein-1. *Int. J. Biochem. Cell Biol.* 36:1882–1886. http://dx.doi.org/10.1016/j.biocel.2003.10.019

Mellman, I., G. Coukos, and G. Dranoff. 2011. Cancer immunotherapy comes of age. *Nature.* 480:480–489. http://dx.doi.org/10.1038/nature10673

Moore, S.J., M.G. Hayden Gephart, J.M. Bergen, Y.S. Su, H. Rayburn, M.P. Scott, and J.R. Cochran. 2013. Engineered knottin peptide enables noninvasive optical imaging of intracranial medulloblastoma. *Proc. Natl. Acad. Sci. USA.* 110:14598–14603. http://dx.doi.org/10.1073/pnas.1311333110

Mulgrew, K., K. Kinneer, X.-T. Yao, B.K. Ward, M.M. Damschroder, B. Walsh, S.-Y. Mao, C. Gao, P.A. Kiener, S. Coats, et al. 2006. Direct targeting of αvβ3 integrin on tumor cells with a monoclonal antibody, Abegrin. *Mol. Cancer Ther.* 5:3122–3129. http://dx.doi.org/10.1158/1535-7163.MCT-06-0356

Murphy, P.A., S. Begum, and R.O. Hynes. 2015. Tumor angiogenesis in the absence of fibronectin or its cognate integrin receptors. *PLoS One.* 10:e0120872. http://dx.doi.org/10.1371/journal.pone.0120872

Nielsen, C.H., R.H. Kimura, N. Withofs, P.T. Tran, Z. Miao, J.R. Cochran, Z. Cheng, D. Felsher, A. Kjær, J.K. Willmann, and S.S. Gambhir. 2010. PET imaging of tumor neovascularization in a transgenic mouse model with a novel 64Cu-DOTA-knottin peptide. *Cancer Res.* 70:9022–9030. http://dx.doi.org/10.1158/0008-5472.CAN-10-1338

Nimmerjahn, F., and J.V. Ravetch. 2005. Divergent immunoglobulin g subclass activity through selective Fc receptor binding. *Science.* 310:1510–1512. http://dx.doi.org/10.1126/science.1118948

O'Day, S., A. Pavlick, C. Loquai, D. Lawson, R. Gutzmer, J. Richards, D. Schadendorf, J.A. Thompson, R. Gonzalez, U. Trefzer, et al. CNTO 95 Investigators. 2011. A randomised, phase II study of intetumumab, an anti-αv-integrin mAb, alone and with dacarbazine in stage IV melanoma. *Br. J. Cancer.* 105:346–352. http://dx.doi.org/10.1038/bjc.2011.183

Pardoll, D.M. 2012. The blockade of immune checkpoints in cancer immunotherapy. *Nat. Rev. Cancer.* 12:252–264. http://dx.doi.org/10.1038/nrc3239

Parvani, J.G., A.J. Galliher-Beckley, B.J. Schiemann, and W.P. Schiemann. 2013. Targeted inactivation of β1 integrin induces β3 integrin switching, which drives breast cancer metastasis by TGF-β. *Mol. Biol. Cell.* 24:3449–3459. http://dx.doi.org/10.1091/mbc.E12-10-0776

Reynolds, A.R., I.R. Hart, A.R. Watson, J.C. Welti, R.G. Silva, S.D. Robinson, G. Da Violante, M. Gourlaouen, M. Salih, M.C. Jones, et al. 2009. Stimulation of tumor growth and angiogenesis by low concentrations of RGD-mimetic integrin inhibitors. *Nat. Med.* 15:392–400. http://dx.doi.org/10.1038/nm.1941

Ries, C.H., M.A. Cannarile, S. Hoves, J. Benz, K. Wartha, V. Runza, F. Rey-Giraud, L.P. Pradel, F. Feuerhake, I. Klaman, et al. 2014. Targeting tumor-associated macrophages with anti-CSF-1R antibody reveals a strategy for cancer therapy. *Cancer Cell.* 25:846–859. http://dx.doi.org/10.1016/j.ccr.2014.05.016

Rosenberg, S.A. 2012. Raising the bar: the curative potential of human cancer immunotherapy. *Sci. Transl. Med.* 4:127ps8. http://dx.doi.org/10.1126/scitranslmed.3003634

Ruffell, B., and L.M. Coussens. 2015. Macrophages and therapeutic resistance in cancer. *Cancer Cell.* 27:462–472. http://dx.doi.org/10.1016/j.ccell.2015.02.015

Schwartz, R.N., L. Stover, and J. Dutcher. 2002. Managing toxicities of high-dose interleukin-2. *Oncology (Williston Park).* 16:11–20.

Sharma, P., and J.P. Allison. 2015. Immune checkpoint targeting in cancer therapy: toward combination strategies with curative potential. *Cell.* 161:205–214. http://dx.doi.org/10.1016/j.cell.2015.03.030

Sheldrake, H.M., and L.H. Patterson. 2014. Strategies to inhibit tumor associated integrin receptors: Rationale for dual and multi-antagonists. *J. Med. Chem.* 57:6301–6315. http://dx.doi.org/10.1021/jm5000547

Shields, R.L., A.K. Namenuk, K. Hong, Y.G. Meng, J. Rae, J. Briggs, D. Xie, J. Lai, A. Stadlen, B. Li, et al. 2001. High resolution mapping of the binding site on human IgG1 for FcγRI, FcγRII, FcγRIII, and FcRn and design of IgG1 variants with improved binding to the FcγR. *J. Biol. Chem.* 276:6591–6604. http://dx.doi.org/10.1074/jbc.M009483200

Siegel, J.P., and R.K. Puri. 1991. Interleukin-2 toxicity. *J. Clin. Oncol.* 9:694–704. http://dx.doi.org/10.1200/JCO.1991.9.4.694

Spranger, S., and T. Gajewski. 2013. Rational combinations of immunotherapeutics that target discrete pathways. *J. Immunother. Cancer.* 1:16. http://dx.doi.org/10.1186/2051-1426-1-16

Strömblad, S., and D.A. Cheresh. 1996. Integrins, angiogenesis and vascular cell survival. *Chem. Biol.* 3:881–885. http://dx.doi.org/10.1016/S1074-5521(96)90176-3

Stupp, R., M.E. Hegi, T. Gorlia, S.C. Erridge, J. Perry, Y.-K. Hong, K.D. Aldape, B. Lhermitte, T. Pietsch, D. Grujicic, et al. CENTRIC study team. 2014. Cilengitide combined with standard treatment for patients with newly diagnosed glioblastoma with methylated MGMT promoter (CENTRIC EORTC 26071-22072 study): a multicentre, randomised, open-label, phase 3 trial. *Lancet Oncol.* 15:1100–1108. http://dx.doi.org/10.1016/S1470-2045(14)70379-1

Topalian, S.L., C.G. Drake, and D.M. Pardoll. 2015. Immune checkpoint blockade: A common denominator approach to cancer therapy. *Cancer Cell.* 27:450–461. http://dx.doi.org/10.1016/j.ccell.2015.03.001

Tzeng, A., B.H. Kwan, C.F. Opel, T. Navaratna, and K.D. Wittrup. 2015. Antigen specificity can be irrelevant to immunocytokine efficacy and biodistribution. *Proc. Natl. Acad. Sci. USA.* 112:3320–3325. http://dx.doi.org/10.1073/pnas.1416159112

van der Flier, A., K. Badu-Nkansah, C.A. Whittaker, D. Crowley, R.T. Bronson, A. Lacy-Hulbert, and R.O. Hynes. 2010. Endothelial α5 and αv integrins cooperate in remodeling of the vasculature during development. *Development.* 137:2439–2449. http://dx.doi.org/10.1242/dev.049551

Ward, P.L., H. Koeppen, T. Hurteau, and H. Schreiber. 1989. Tumor antigens defined by cloned immunological probes are highly polymorphic and are not detected on autologous normal cells. *J. Exp. Med.* 170:217–232. http://dx.doi.org/10.1084/jem.170.1.217

Weis, S.M., and D.A. Cheresh. 2011a. Tumor angiogenesis: Molecular pathways and therapeutic targets. *Nat. Med.* 17:1359–1370. http://dx.doi.org/10.1038/nm.2537

Weis, S.M., and D.A. Cheresh. 2011b. αV integrins in angiogenesis and cancer. *Cold Spring Harb. Perspect. Med.* 1:a006478. http://dx.doi.org/10.1101/cshperspect.a006478

Wolpe, S.D., and A. Cerami. 1989. Macrophage inflammatory proteins 1 and 2: Members of a novel superfamily of cytokines. *FASEB J.* 3:2565–2573.

Zhu, E.F., S.A. Gai, C.F. Opel, B.H. Kwan, R. Surana, M.C. Mihm, M.J. Kauke, K.D. Moynihan, A. Angelini, R.T. Williams, et al. 2015. Synergistic innate and adaptive immune response to combination immunotherapy with anti-tumor antigen antibodies and extended serum half-life IL-2. *Cancer Cell.* 27:489–501. http://dx.doi.org/10.1016/j.ccell.2015.03.004